Multiple-trapping transient currents in thin dielectric layers with enhanced trap density in the near-contact regions

1990 J. Phys.: Condens. Matter 2 3547

(http://iopscience.iop.org/0953-8984/2/15/011)

J. Phys.: Condens. Matter 2 (1990) 3547–3552. Printed in the UK

Multiple-trapping transient currents in thin dielectric layers with enhanced trap density in the near-contact regions

J Rybicki, M Chybicki, S Feliziani† and G Mancini†
Technical University of Gdańsk, Faculty of Technical Physics and Applied Mathematics, Majakowskiego 11/12, 80–952 Gdańsk, Poland

Received 8 June 1989, in final form 24 November 1989

Abstract. We present several illustrative multiple-trapping current–time characteristics in thin dielectric layers with enhanced trap concentration in the near-contact regions. Such a spatial trap distribution, for different energy trap distributions, leads to a variety of different non-typical shapes of the characteristics. The results have been obtained with the aid of a Monte Carlo simulation for conditions corresponding to the typical time-of-flight method.

1. Introduction

Even very carefully prepared thin dielectric layers can be hardly believed to have an ideally homogeneous space trap distribution, at least in the near-contact regions. The enhanced trap density in the near-contact regions may originate, for example, from diffusion of atoms from contacts or ambient atmosphere, chemical reactions or lattice constant mismatching, and may extend for some distance into the layer.

In this paper we present some illustrative Monte Carlo results showing that the presence of the enhanced density of trapping centres strongly localised in the near-contact regions can lead to a variety of different non-typical shapes of the current–time characteristics and can completely cover the effects due to bulk traps. The spatial non-homogeneity of the trap distribution may be in general one of the factors leading to distinct discrepancies between the experimental results (see, e.g., Pfister and Scher 1978, Muller-Horsche *et al* 1987, Di Marco *et al* 1989) and theoretical predictions (see, e.g., Scher and Montroll 1975). Thus a study of pure effects arising from an x-dependent trap distribution could help the experimentalist to interpret data.

After description of the assumed model spatial and energy trap distribution (section 2) and of the simulation algorithm (section 3), we present and discuss the numerical results (section 4), concluding the paper with some final remarks (section 5).

2. Model trap distribution

The energy and spatial trap distribution is here assumed to be as follows:

$$N_t(x, \mathscr{E}) = N_0 f_0(\mathscr{E}) + N_l S_l(x) f_l(\mathscr{E}) + N_r S_r(x) f_r(\mathscr{E}) \tag{1}$$

where x is the spatial coordinate ($0 \leq x \leq L$, where L is the layer thickness) and $\mathscr{E}$ is the

† Present address: Istituto di Matematica e Fisica, Universita di Camerino, Camerino, Italy.

0953-8984/90/153547 + 06 $03.50

trap depth measured down from the bottom of the conduction band. The trap distribution (1) is written as a sum of three fractions of traps: $N_0 f_0(\mathscr{E})$ represents an x-independent bulk trap distribution, and $(N_l S_l(x) f_l(\mathscr{E})$ and $N_r S_r(x) f_r(\mathscr{E})$ describe the near-surface enhanced trap density. The subscripts l and r refer to the left and right surfaces of the layer, so that the second and the third terms in (1) correspond to the traps localised near $x = 0$ and $x = L$, respectively. The functions f_0, f_l and f_r describing the energy trap distributions of corresponding trap fractions are normalised to unity ($\int_0^\infty f_i(\mathscr{E})\,\mathrm{d}\mathscr{E} = 1$, $i = 0, l, r$). Thus the total trap density is given by $N_t^{tot}(x) = N_0 + N_l S_l(x) + N_r S_r(x)$. $S_l(x)$ and $S_r(x)$ are dimensionless shape functions of the near-contact spatial distributions of traps, normalised to unity in the sense $S_l(0) = 1$ and $S_r(L) = 1$. Because of the assumed strong localisation of additional traps near the layer surfaces, the total trap densities in $x = 0$ and $x = L$ are $N_t^{tot}(0) = N_0 + N_l$ and $N_t^{tot}(L) = N_0 + N_r$. We shall assume the f-functions to be exponential in energy:

$$f_i(\mathscr{E}) \sim \exp[-(\mathscr{E} - \mathscr{E}_i)/kT_i] \tag{2}$$

where $\mathscr{E}_i$ are the cut-off energies of trap distribution components, $i = 0, l, r$ (no traps in the interval $(0, \mathscr{E}_i)$) and T_i are the characteristic temperatures. The spatial shape functions S_l and S_r are assumed to be

$$S_l(x) = \exp(-x/D_l) \tag{3}$$

$$S_r(x) = \exp[-(L - x)/D_r] \tag{4}$$

where D_l and D_r are parameters ($D_l, D_r \ll L$). The energy and spatial distributions (2)–(4) cover a wide class of materials of which the layer and contacts are made and should be sufficiently representative to illustrate the specific features of transient currents in the dielectric layers with enhanced trap concentrations in the near-contact regions.

3. Simulation algorithm

Transient currents have been calculated with the aid of Monte Carlo simulation. The simulation has been performed according to an algorithm which is the generalisation of that proposed by Silver *et al* (1971) and used previously by Rybicki and Chybicki (1988, 1989). The algorithm does not take into account space-charge effects and diffusion. A single trapping–detrapping event is described by random values of the trapping time $\tau(x)$ (lifetime in the conduction band), the depth $\mathscr{E}$ of the trap and the detrapping time $\tau_d(\mathscr{E})$ (dwell time in the trap). The random values $\tau(x)$, $\mathscr{E}$ and $\tau_d(\mathscr{E})$ are generated according to their distribution functions F, which have a uniform distribution in the interval (0, 1) (see, e.g., Dwass 1970). The distribution functions are

$$F_{\tau(x)} = \frac{1}{\bar{\tau}(x)} \int_0^{\tau(x)} \exp\left(-\frac{\tau'}{\bar{\tau}(x)}\right) \mathrm{d}\tau' \tag{5}$$

$$F_{\mathscr{E}} = \int_0^{\mathscr{E}} [N_0 f_0(\mathscr{E}') + N_l S_l(x) f_l(\mathscr{E}') + N_r S_r(x) f_r(\mathscr{E}')] \times [N_0 + N_l S_l(x) + N_r S_r(x)]^{-1}\,\mathrm{d}\mathscr{E}' \tag{6}$$

$$F_{\tau_d} = \frac{1}{\bar{\tau}_d(\mathscr{E})} \int_0^{\tau_d} \exp\left(-\frac{\tau_d'}{\bar{\tau}_d(\mathscr{E})}\right) \mathrm{d}\tau_d'. \tag{7}$$

The random values of $\tau(x)$, $\mathscr{E}$ and $\tau_d(\mathscr{E})$ are obtained by solving the equations $F_{\tau(x)} = X$, $F_{\mathscr{E}} = Y$ and $F_{\tau_d} = Z$, where X, Y and Z are random numbers from the interval (0, 1). In equations (5)–(7), $\bar{\tau}(x)$ is the mean trapping time in x:

$$[\bar{\tau}(x)]^{-1} = C[N_0 + N_l S_l(x) + N_r S_r(x)] \tag{8}$$

where C is the capture coefficient given by σv_{th} (σ is the trapping cross section and v_{th} the thermal velocity) and $\bar{\tau}_d(\mathscr{E})$ is the mean detrapping time from the trap of depth $\mathscr{E}$:

$$[\bar{\tau}_d(\mathscr{E})]^{-1} = \nu \exp(-\mathscr{E}/kT) \tag{9}$$

where ν is the frequency factor, k the Boltzmann constant and T the temperature. The ith distance Δx_i travelled by the carrier between two successive trappings is $\Delta x_i = \mu E \tau_i(x)$ (μ is the microscopic mobility and E the external electric field), and the elementary contribution $\Delta j_i(t)$ to the current in the external circuit flowing during time $\tau_i(x)$ is $\Delta j_i(t) = q\mu E/L$ (q is the elementary charge and $t = \Sigma_i (\tau_i + \tau_{di})$, τ_i and τ_{di} being ith random trapping and detrapping times, respectively). Each carrier starts its random motion at $x = 0$ at $t = 0$, which corresponds to the generation of a very thin (compared with the layer thickness) wall of carriers at one of the contacts by a pulse of duration short in comparison with the time scale of the transient. The trapping–detrapping events are repeated until the carrier reaches $x = L$, where $x = \Sigma_i \Delta x_i$. The results were obtained by averaging random motions of 5×10^3–10^4 individual carriers.

4. Numerical results and discussion

Figure 1 presents the results for $N_l = N_r = 10^3 N_0$ with $D_l = D_r$ in the range $0.001L$–$0.02L$ (other parameters are specified in the caption). The sharpness of the current peak increases as the parameter $D_{r,l}/L$ decreases. For $D_{l,r}/L = 0.001$ the relative increase in the current for $\alpha_i = 0.75$, $i = 0$, l, r ($\alpha_i = T/T_i$, where T is the layer temperature) is over two orders of magnitude. The more dispersive the transport (smaller α_i), the smaller is the relative current increase (e.g. for $\alpha_i = 0.25$ and $D_{l,r}/L = 0.001$, it is less than one order of magnitude (cf Rybicki and Chybicki 1988, 1989)). The shape of the current transients A–C and E in figure 1 are determined entirely by the trap distribution near the injecting contact. If the enhanced trap density occurs only in the vicinity of $x = 0$ ($N_r = 0$), the current shape is almost identical (shifted towards shorter times by a few line thicknesses in the scale applied in the figure) with that for $N_l = N_r$. On the other hand, if $N_l = 0$ and $N_r = 10^3 N_0$, the current shape hardly differs from the case $N_l = N_r = 0$ (curve D in figure 1). Thus, curves C (corresponding approximately to the case $N_r = 0, N_l = 10^3 N_0$) and D (corresponding to $N_r = 10^3 N_0, N_l = 0$) show a polarity dependence of transient currents in a layer with enhanced trap density near only one contact.

Because of the dominating role of the trap distribution in the vicinity of $x = 0$, we have performed further calculations for $N_r = 0$, shortening the computer time by eliminating many near-right-hand-side-contact trapping events, which hardly affects the shapes of transients. All the curves in figures 2 and 3 were calculated for $D_l/L = 0.005$.

Figure 2 corresponds to a very narrow energy distribution of bulk traps ($\alpha_0 = 2.0$), leading to non-dispersive transport (curve A). The near-contact energy trap distribution is characterised by $\alpha_l = 0.75$. As easily seen, even a relatively high density N_l of sufficiently shallow traps does not perturb the non-dispersive bulk transport (curve B). On the other hand, a much lower density N_l of sufficiently deep traps can lead to a very complicated transient (curve E). The first slow current decay is due to the absorption of

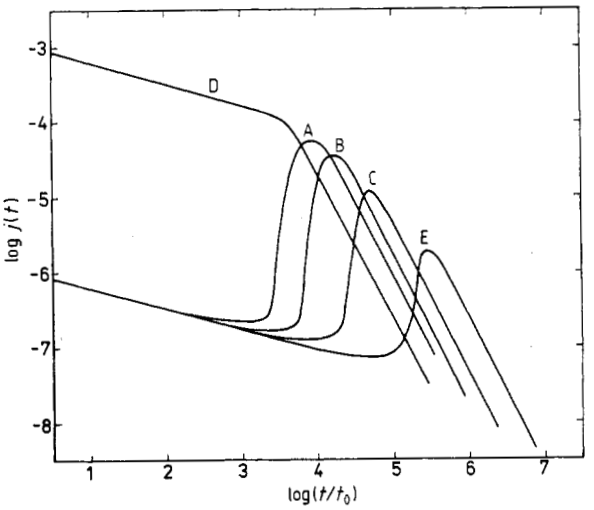

Figure 1. Transient currents for the trap distribution (1)–(4) as a function of the width of the near-contact enhanced trap density ($\alpha_i = 0.75$; $\nu \exp(-\mathscr{E}_i/kT) = 5 \times 10^3$ s^{-1}; $i = 0, l, r$; $\sigma v_{th} = 10^{-13}$ cm^3 s^{-1}): curve A, $N_0 = 10^{19}$ cm^{-3}, $N_l = N_r = 10^{22}$ cm^{-3}, $D_l/L = D_r/L = 0.001$; curve B, $N_0 = 10^{19}$ cm^{-3}, $N_c = N_r = 10^{22}$ cm^{-3}, $D_l/L = D_r/L = 0.002$; curve C, $N_0 = 10^{19}$ cm^{-3}, $N_l = N_r = 10^{22}$ cm^{-3}, $D_l/L = D_r/L = 0.005$; curve D, $N_l = 0$, $N_0 = 10^{19}$ cm^{-3}, $N_r = 10^{22}$ cm^{-3}, $D_r/L = 0.005$; curve E, $N_0 = 10^{19}$ cm^{-3}, $N_l = N_r = 10^{22}$ cm^{-3}, $D_l/L = D_r/L = 0.02$. The average numbers of trapping–detrapping events over the layer thickness for curves A, B, C, D and E are approximately 3000, 5000, 11 000, 6000 and 21 000, respectively. Curves C and D almost coincide with those calculated for $N_r = 0$, $N_0 = 10^{19}$ cm^{-3}, $N_l = 10^{22}$ cm^{-3}, $D_l/L = 0.005$, and for $N_l = N_r = 0$, $N_0 = 10^{19}$ cm^{-3}, respectively.

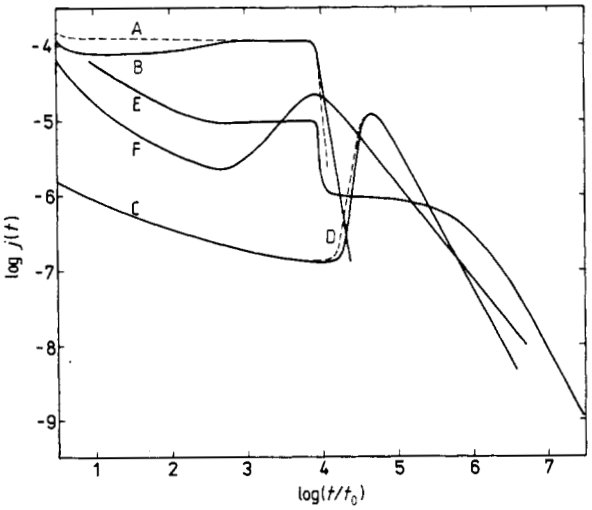

Figure 2. Transient currents for trap distribution (1)–(4) ($N_r = 0$; $D_l/L = 0.005$; $\alpha_0 = 2$; $\nu \exp(-\mathscr{E}_0/kT) = 2.3 \times 10^2$ s^{-1}; $\sigma v_{th} = 10^{-13}$ cm^3 s^{-1}): curve A, $N_l = 0$, $N_0 = 10^{19}$ cm^{-3}; curve B, $N_l = 5 \times 10^{21}$ cm^{-3}, $N_0 = 10^{19}$ cm^{-3}, $\alpha_l = 0.75$, $\mathscr{E}_l = \mathscr{E}_0 - 10\,kT$; curve C, $N_l = 10^{21}$ cm^{-3}, $N_0 = 10^{19}$ cm^{-3}, $\alpha_l = 0.75$, $\mathscr{E}_l = \mathscr{E}_0$; curve D, $N_l = 10^{21}$ cm^{-3}, $N_0 = 0$, $\alpha_l = 0.75$, $\mathscr{E}_l = \mathscr{E}_0$; curve E, $N_l = 5 \times 10^{18}$ cm^{-3}, $N_0 = 10^{19}$, $\alpha_l = 0.75$, $\mathscr{E}_l = \mathscr{E}_0 + 10\,kT$; curve F, $N_l = 10^{21}$ cm^{-3}, $N_0 = 10^{19}$ cm^{-3}, $\alpha_l = 0.333$, $\mathscr{E}_l = \mathscr{E}_0 - 10\,kT$.

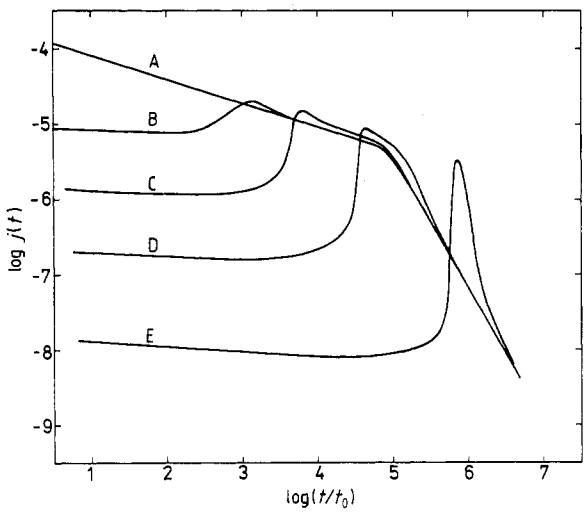

Figure 3. Transient currents for trap distribution (1)–(4) ($N_r = 0$, $D_l/L = 0.005$; $\alpha_0 = 0.75$; $\alpha_l = 2$; $\nu \exp(-\mathscr{E}_0/kT) = 2.3 \times 10^2\,s^{-1}$; $\sigma v_{th} = 10^{-13}\,cm^3\,s^{-1}$; $N_0 = 10^{19}\,cm^{-3}$): curve A, $N_l = 0$; curve B, $N_l = 10^{21}\,cm^{-3}$, $\mathscr{E}_l = \mathscr{E}_0 - 2\,kT$; curve C, $N_l = 10^{21}\,cm^{-3}$, $\mathscr{E}_l = \mathscr{E}_0$; curve D, $N_l = 10^{21}\,cm^{-3}$, $\mathscr{E}_l = \mathscr{E}_0 + 2\,kT$; curve E, $N_l = 10^{21}\,cm^{-3}$, $\mathscr{E}_l = \mathscr{E}_0 + 5\,kT$.

the carriers in deep traps near $x = 0$. The carriers which avoided deep trapping contribute to non-dispersive bulk transport, with their effective time of flight (about $10^4 t_0$, where t_0 is the trap-free time of flight). For longer times, detrapping from the near-contact deep traps occurs, leading to a lower current of dispersive character, with the 'second' effective time of flight (about $2 \times 10^6 t_0$), and a $t^{-(1+\alpha)}$ decay in the post-time-of-flight region. Curves C and D in figure 2 show the effect of covering the action of bulk traps by those strongly localised in the vicinity of $x = 0$.

Figure 3 shows some examples of results obtained for the near-contact traps with $\alpha_l = 2.0$, superimposed on the bulk traps characterised by $\alpha_0 = 0.75$. The reference curve A corresponds to $N_l = 0$. The subsequent transients B–E correspond to different cut-off energies $\mathscr{E}_l$ (see caption). The portions of transients left of the current maximum correspond to the non-dispersive transport of an almost Gaussian carrier packet in the region of enhanced trap density (cf Rybicki and Chybicki 1989), perturbed with the carrier absorption in deep traps (slight current decrease seen in the flat portions). The packet, after reaching the $N_l(x) \simeq 0$ region, becomes a Scher–Montroll dispersive packet, leading to dispersive current decay. The dispersive bulk transport is thus delayed by the time necessary to leave the enhanced-trap-density region. The shape of the final current in curve E is in fact very similar to the reference curve A, plotted with its time argument shifted towards longer times by the duration of carrier transport through the near-contact region.

5. Concluding remarks

Obviously, more complicated spatial and energy trap distributions may lead to correspondingly more complicated transients. Moreover, there is no one-to-one relation

between the trap distributions and current shapes; trap distributions, which are completely different from the physical point of view, may lead to almost identical transients. The above results show pure effects due to the presence of traps strongly localised in the near-contact regions in two limiting cases: narrow-energy near-contact distributions superimposed onto a wide-energy bulk distribution; wide-energy near-contact distributions superimposed onto a narrow-energy bulk distribution. Thus one can also gain some insight into the current shapes in intermediate or more complicated cases.

Acknowledgment

The support from CPBP 0108 E is kindly acknowledged.

References

Di Marco P G, Kalinowski J, Giro G and Rybicki J 1989 *Thin Solid Films* **181** at press
Dwass M 1970 *Probability and Statistics. An Undergraduate Course* (New York: Benjamin) p 274
Muller-Horsche E, Haarer D and Scher H 1987 *Phys. Rev.* B **33** 1273
Pfister G and Scher H 1978 *Adv. Phys.* **27** 747
Rybicki J and Chybicki M 1988 *J. Phys. C: Solid State Phys.* **21** 3073
—— 1989 *J. Phys.: Condens. Matter* **1** 4623
Scher H and Montroll E W 1975 *Phys. Rev.* B **12** 2455
Silver M, Dy K S and Huang I L 1971 *Phys. Rev. Lett.* **27** 21